GPS Data Analysis

Of all GPS stations on the Pacific Plate, we exclude most stations on Hawaii's Big Island, because of volcanic processes there, and several stations near the Tonga subduction zone that may be affected by elastic strain accumulation. We also only consider stations with >3.5 years of data. All data are processed with the GIPSY software package and we derive velocities from position time-series in the ITRF2008 reference frame. Velocities are derived while estimating annual and semi-annual motions, and velocity uncertainties are estimated assuming a noise model containing white and flicker noise (see table). We solve for a rigid-body rotation using most velocities (See Electronic Table 1), with notable exceptions being the stations on Chatham Island (CHAT, CHTI) and the station on Guadalupe Island (GUAX), off the coast of Mexico, which is the only station on relatively young lithosphere. The residual velocities are shown in Fig. 1C. The table also shows the predicted velocities at the GPS stations (in the same reference frame).

Earthquake Catalog

We use the well-located events from 1963-2008 determined by Engdahl et al. (1998). We adopted a completeness magnitude $m_b \geq 5.0$ from Okal and Sweet (Okal and Sweet, 2007) from their analysis of Pacific plate events. Given the epicenter uncertainty (95% confidence), we remove any event that could have occurred outside the Pacific plate polygon. To ensure that we do not accidentally include ridge-transform events, we also exclude events in <5 Ma old lithosphere. Earthquake epicenters of Engdahl et al. (1998) were shown to be not very accurate near the Udintsev and Eltanin transform faults (Okal and Langenhorst, 2000), so we excluded those too. We then only use events <40 km deep, remove events near the subduction zones in the east and north (including those that can be considered “bending events”), remove events in grid cells that have an average bathymetric depth less than 2 km (to avoid including volcanic events), remove additional events around Hawaii's Big Island, remove events that occurred on Mururoa Atoll and that presumably were nuclear explosions, remove events due to the Gulf Alaska sequence between 1987 and 1992, and remove those that were in notable swarms (1981-1983 near the Gilbert Islands (Lay and Okal, 1983), 1991-1992 300km west of the East Pacific Rise (Hung and Forsyth, 1996), 1984-1986 SE of Baja California (Wiens and Okal, 1987), and 1976-1983 500 km NE of Pitcairn Island (Okal et al., 1980)). Removal of these swarms is needed to ensure that the catalog is time-independent.

References

Engdahl, E.R., van der Hilst, R., and Buland, R., 1998, Global teleseismic earthquake relocation with improved travel times and procedures for depth determination: Bulletin of the Seismological Society of America, v. 88, no. 3, p. 722–743.

Hung, S.-H., and Forsyth, D.W., 1996, Non-double-couple focal mechanisms in an oceanic, intraplate earthquake swarm: Application of an improved method for comparative event, moment tensor determination: Journal of Geophysical Research: Solid Earth, v. 101, no. B11, p. 25347–25371, doi: 10.1029/96JB02286.

Lay, T., and Okal, E., 1983, The Gilbert Islands (Republic of Kiribati) earthquake swarm of 1981–1983: Physics of the Earth and Planetary Interiors, v. 33, no. 4, p. 284–303, doi: 10.1016/0031-9201(83)90046-8.

Okal, E.A., and Langenhorst, A.R., 2000, Seismic properties of the Eltanin Transform System, South Pacific: Physics of the Earth and Planetary Interiors, v. 119, no. 3–4, p. 185–208, doi: 10.1016/S0031-9201(99)00169-7.

Okal, E.A., and Sweet, J.R., 2007, Frequency-size distributions for intraplate earthquakes (S. Stein & S. Mazzotti, Eds.): Geological Society of America Special Papers, v. 425, p. 59–71, doi: 10.1130/2007.2425(05).

Okal, E.A., Talandier, J., Sverdrup, K.A., and Jordan, T.H., 1980, Seismicity and tectonic stress in the south-central Pacific: Journal of Geophysical Research: Solid Earth, v. 85, no. B11, p. 6479–6495, doi: 10.1029/JB085iB11p06479.

Wiens, D.A., and Okal, E.A., 1987, Tensional intraplate seismicity in the Eastcentral Pacific: Physics of the Earth and Planetary Interiors, v. 49, no. 3–4, p. 264–282, doi: 10.1016/0031-9201(87)90029-X.

					ITRF2008				GPS-FIXED		MODEL_1		MODEL_2	
SITE	LON	LAT	START	END	VE	VN	SDVE	SDVN	VE	VN	VE	VN	VE	VN
CHAT*	-176.566	-43.956	1996.0	2012.2	-40.58	33.24	0.13	0.11	0.56	-0.10	0.55	-0.44	0.67	-0.62
CHTI*	-176.617	-43.735	2007.9	2014.0	-41.27	32.76	0.29	0.30	0.06	-0.57	0.55	-0.44	0.66	-0.62
CKIS	-159.801	-21.201	2001.7	2014.0	-62.40	35.03	0.26	0.23	0.07	0.13	0.07	-0.05	0.13	-0.06
COOK	-159.812	-21.201	1998.2	2012.0	-63.15	35.28	0.22	0.19	-0.68	0.38	0.07	-0.05	0.13	-0.06
FAA1	-149.614	-17.555	2006.8	2014.0	-66.19	34.61	0.40	0.33	-0.42	0.21	0.01	0.07	0.06	0.09
GAMB	-134.965	-23.130	2000.3	2010.8	-67.51	31.96	0.19	0.14	-0.13	0.17	0.03	0.30	-0.02	0.37
GUAX*	-118.290	28.884	2001.4	2005.2	-47.23	25.29	0.36	0.42	0.46	-1.03	-0.14	-0.30	-0.20	-0.40
HNLC	-157.865	21.303	1997.5	2013.9	-62.57	34.62	0.16	0.13	-0.37	-0.27	-0.03	-0.09	-0.02	-0.13
KIRI	172.923	1.355	2002.6	2014.0	-67.75	31.25	0.22	0.17	-0.26	0.36	-0.01	0.02	-0.05	0.03
KOKO	-159.758	21.983	1996.1	2014.0	-62.18	35.17	0.11	0.09	0.15	0.27	-0.02	-0.09	-0.01	-0.12
KOKB	-159.665	22.126	1996.0	2014.0	-62.16	34.66	0.18	0.13	0.08	-0.24	-0.02	-0.09	-0.01	-0.12
KRTM	-157.448	2.047	1997.2	2014.0	-67.16	34.77	0.13	0.10	-0.13	-0.12	-0.09	-0.05	-0.06	-0.05
KWJ1	167.730	8.722	1996.2	2002.6	-68.79	29.34	0.25	0.24	0.43	0.04	0.02	0.04	-0.01	0.05
MAJB	171.365	7.119	2007.4	2014.0	-68.67	30.54	0.34	0.29	0.04	0.10	0.01	0.02	-0.02	0.04
MAUI	-156.257	20.707	1999.0	2014.0	-61.89	34.62	0.12	0.11	0.23	-0.24	-0.04	-0.09	-0.03	-0.13
MCIO	153.979	24.290	1996.0	2011.2	-71.72	23.70	0.20	0.21	-0.10	-0.25	0.10	0.09	0.07	0.12
MKEA	-155.456	19.801	1996.7	2014.0	-62.49	34.96	0.11	0.09	-0.15	0.14	-0.04	-0.09	-0.04	-0.13
NAUR	166.926	-0.552	2003.5	2014.0	-66.70	29.73	0.25	0.21	0.22	0.69	-0.01	0.05	-0.06	0.07
PAPE*	-149.573	-17.533	2004.0	2014.0	-66.67	34.21	0.20	0.18	-0.89	-0.19	0.01	0.07	0.05	0.09
POHN	158.210	6.960	2003.3	2014.0	-69.48	25.14	0.23	0.22	-0.01	-0.62	0.02	0.08	-0.01	0.10
TAH1	-149.606	-17.577	2000.6	2014.0	-65.83	34.33	0.31	0.15	-0.07	-0.07	0.01	0.07	0.06	0.09
TARW	172.923	1.355	1999.1	2013.1	-67.10	30.97	0.14	0.14	0.39	0.07	-0.01	0.02	-0.05	0.03
TBTG*	-149.476	-23.342	2009.4	2013.8	-64.44	33.69	0.51	0.37	-0.45	-0.69	0.09	0.10	0.15	0.12
THTO	-149.606	-17.577	1996.0	2014.0	-65.80	34.40	0.18	0.14	-0.03	-0.01	0.01	0.07	0.06	0.09
TRUK	151.887	7.447	1996.5	2002.7	-70.11	23.20	0.67	0.43	-0.15	0.19	0.03	0.10	-0.01	0.13
TUVA	179.197	-8.525	2001.9	2009.7	-63.92	32.16	0.32	0.21	0.56	-0.33	-0.06	-0.03	-0.12	-0.01
ZHN1	-157.921	21.313	2003.2	2014.0	-62.23	34.65	0.26	0.23	-0.02	-0.25	-0.03	-0.09	-0.02	-0.13

All velocity units are in mm/yr. Stations noted with an * were not used in the estimation of a rigid-body rotation

KOK0 is the concatenation of KOK1 and KOK5

MCI0 is the concatenation of MARC and MCIL

THT0 is the concatenation of PAMA, TAHI, and THTI

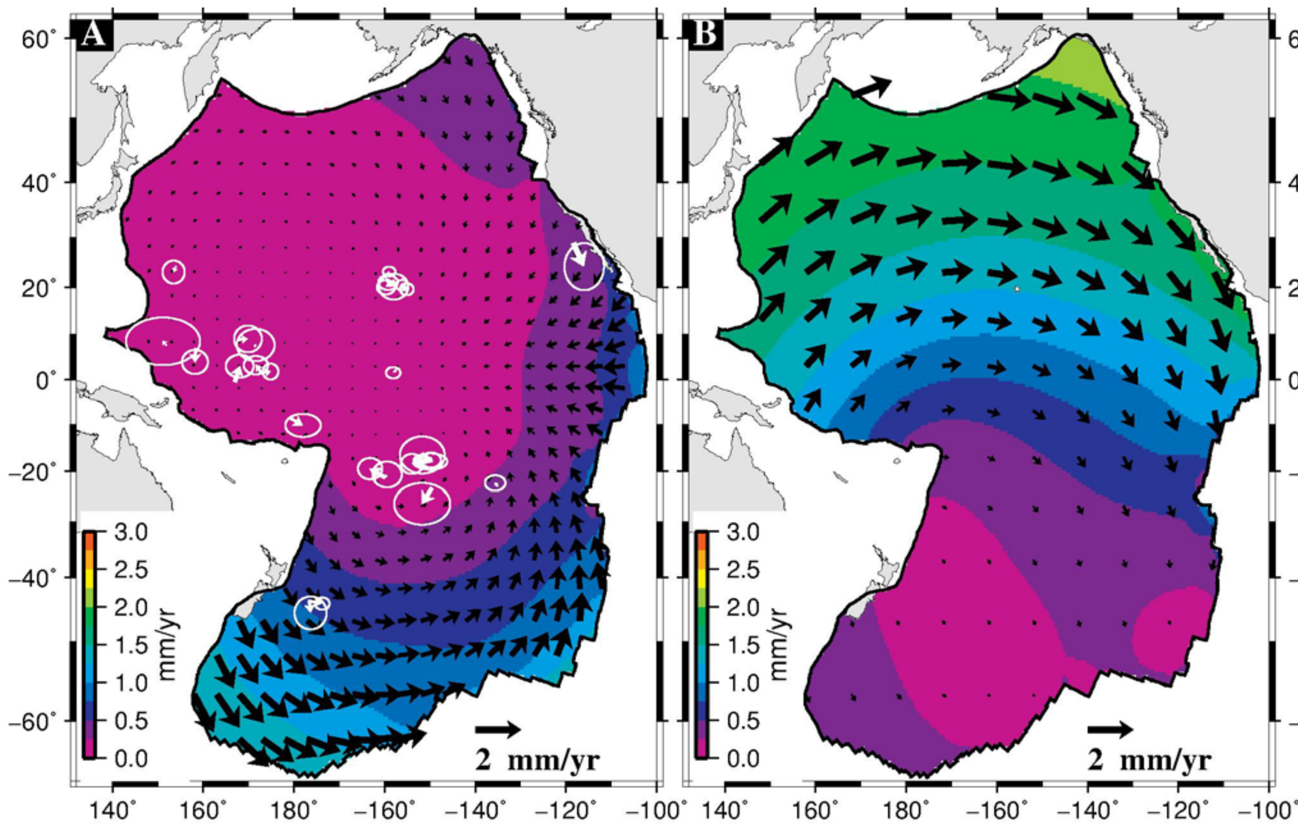

Figure DR1. A) Residual GPS velocities (white vectors), after removal of rigid-body rotation, with 95% confidence error ellipses. Black vectors and contours are predicted velocities from thermal contraction (Model 1) are shown in the same frame as GPS, B) Predicted velocities (vectors and contours) from thermal contraction (Model 1) relative to the 0.78 Ma isochron along the Pacific-Antarctic Ridge.

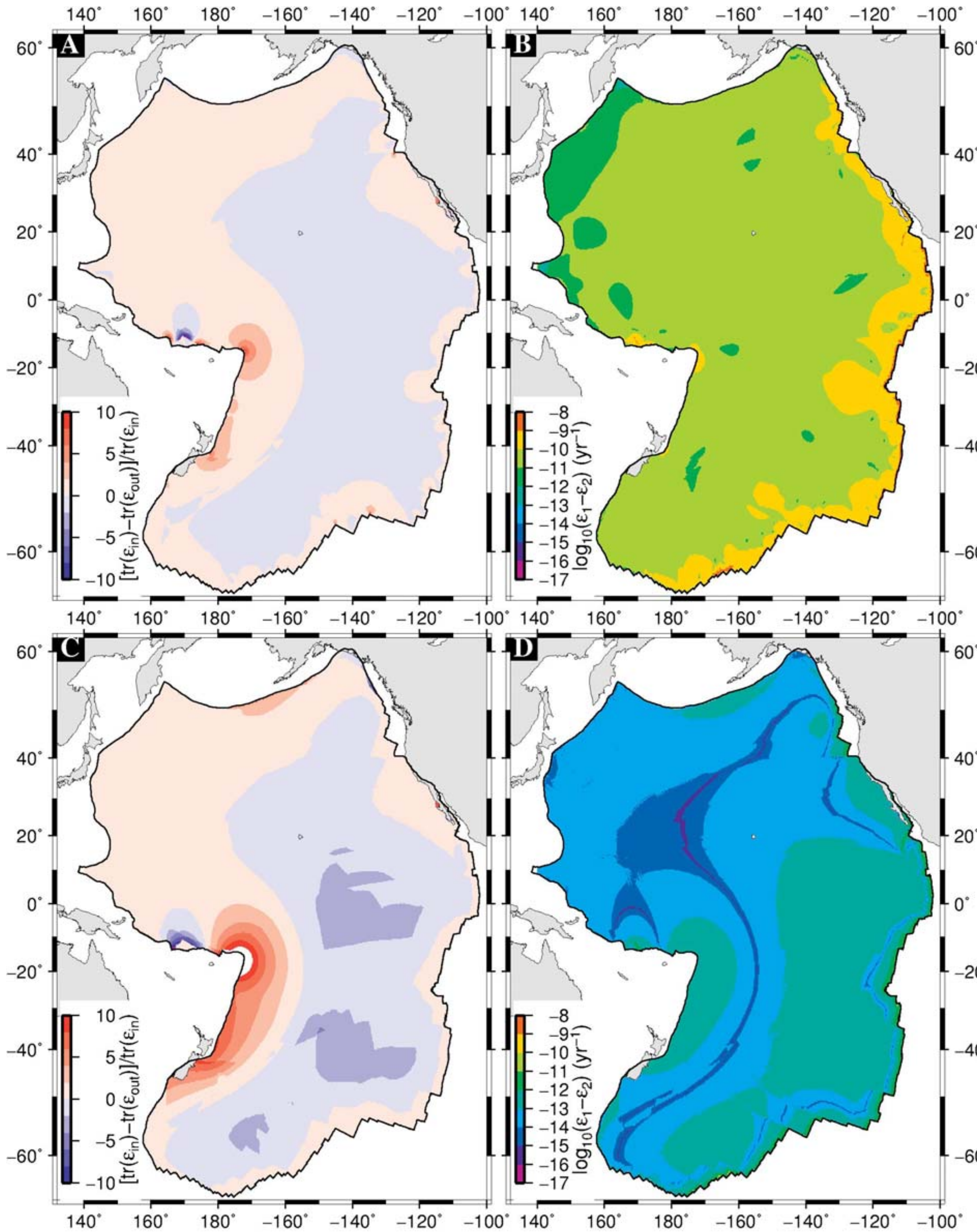

Figure DR2. A) Relative difference between the trace of the input strain rate tensor (i.e., bi-axial shortening) and that of the modeled strain rate tensor for Model 1. This result is a measure on how well this model maintains the rate of strain that is expected based on age. B) Shear component of the modeled strain rate tensor, defined as difference between largest and smallest eigenvalue, for Model 1. This result is a measure on how well the this model maintains the bi-axial constraint (i.e., how much shear is introduced). C) same as A but for Model 2, D) same as B but for Model 1.